JOURNAL OF PHYSICAL ORGANIC CHEMISTRY
J. Phys. Org. Chem. 2007; **20:** 1058–1071
Published online 14 September 2007 in Wiley InterScience
(www.interscience.wiley.com) DOI: 10.1002/poc.1255

A computational study into the reactivity of epichlorohydrin and epibromohydrin under acidic conditions in the gas phase and aqueous solution

E. S. Shields[†] and G. N. Merrill*

Department of Chemistry, University of Texas at San Antonio, Texas 78249-0698, USA

Received 8 May 2007; revised 19 July 2007; accepted 19 July 2007

ABSTRACT: *Ab initio* molecular orbital calculations have been carried out upon epichlorohydrin and epibromohydrin at the Hartree–Fock (HF) and Møller–Plesset (MP2) levels of theory to explore the reactivity of these species with respect to nucleophilic attack by water under acidic conditions in the gas phase and aqueous solution. These results suggest that nucleophilic attack occurs preferentially at the epoxy carbon atoms in both the gas phase and aqueous solution. These results are in contrast to those found for nucleophilic attack under basic conditions, where attack at the halocarbon atom is competitive with that at the epoxy carbon atoms. Copyright © 2007 John Wiley & Sons, Ltd. *Supplementary electronic material for this paper is available in Wiley InterScience at http://www.mrw.interscience.wiley.com/suppmat/0894-3230/suppmat/*

KEYWORDS: epibromohydrin; epichlorohydrin; water; reaction mechanism; gas phase; solution; *ab initio* modeling

INTRODUCTION

In two previous papers,[1] we reported the results of our computational investigations into the reactivities of epihalohydrins in the gas phase and aqueous solution under basic conditions. Specifically, we addressed the question: Does nucleophilic attack by an archetypal hard nucleophile (hydroxide, OH^-) occur at the C1 methylene, C2 methine, or C3 methylene positions of epichlorohydrin (**Ia**) and epibromohydrin (**Ib**)?

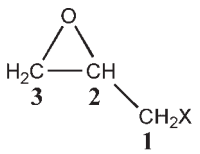

Ia, X = Cl Ib, X = Br

A computational approach to the study of the gas-phase behavior of these systems is necessitated, as experimental approaches (e.g., mass spectrometry) are incapable of conclusively determining the specific sites of nucleophilic attack.

In the gas phase, attack at the C1 atom was found to be about three times more favorable than that at the C3 atom for epibromohydrin. Attack at the C3 atom was, however, determined to be nearly 15 times more likely for epichlorohydrin. In both cases, nucleophilic attack at the C2 position was found to be inconsequential, occurring in less than one percent of the reactions in the gas phase. These results clearly demonstrate that improving the quality of the leaving group (from Cl^- to Br^-) increases the likelihood of attack at the halocarbon atom.

In the polar, aprotic solvent acetone, attack at the C1 position was effectively shutdown for both epihalohydrins; C3 attack was approximately 200 times more favorable. Nucleophilic attack at the C2 position was, once again, found not to occur to any great extent. These results were explained by the preferential stabilization of the C3 transition state by the solvent.

These computational results are in good agreement with those obtained experimentally.[2–7] More importantly, the computational work provided detailed mechanisms for the intrinsic (i.e., gas phase) reactivity of these industrially important systems and offered insights into the rational selection of solvent system to control reactivity.

In this final paper, we report the results of our computational study into the reactivity of epichlorohydrin

**Correspondence to:* G. N. Merrill, One UTSA Circle, Department of Chemistry, University of Texas at San Antonio, San Antonio, TX 78249-0698, USA.
E-mail: grant.merrill@utsa.edu
[†]Present Address: Department of Chemistry and Biochemistry, University of Texas at Austin, Austin, Texas 78712-0165, USA.

and epibromohydrin under acidic conditions both in the gas phase and aqueous solution. Here, water (H_2O) served as the nucleophile and the protonated epihalohydrins were the substrates. It will be shown that the reactivities of epihalohydrins are very pH-dependent. This work also serves to fill a gap in the experimental literature regarding these chemically interesting systems.

COMPUTATIONAL METHODS

The following computational procedure was employed in carrying out the current calculations.

1. Structures were fully optimized at the restricted Hartree–Fock (RHF)[8] level of theory with the double split-valence 6-31G basis set[9] to which sets of d-polarization[10] and sp-diffuse[11] functions were added to all atoms save hydrogen; that is, the 6-31 + G(d) basis set. Structural convergence was achieved when the maximum and root-mean-square of the gradients fell below 0.012 and 0.004 kcal mol^{-1} Å^{-1}, respectively (1 kcal = 4.184 kJ and 1 Å = 10^{-10} m). All relevant stationary points were located and fully characterized.
2. Hessian matrices were computed for all stationary points (minima and transition states) at the HF/6-31 + G(d) level. The absence of negative eigenvalues confirmed a stationary point as a minimum, while the presence of a single negative eigenvalue established the stationary point as a transition state.
3. Enthalpic and entropic corrections were calculated for all stationary points using standard statistical mechanical formulae.[12] All vibrational frequencies, derived from the HF/6-31 + G(d) Hessian matrices, were scaled by an empirical factor of 0.8953 to compensate for the known overestimation of these values by the harmonic approximation at the RHF level with double-zeta quality bases.[13] Thermodynamic corrections were made to 1 atm and 298 K.
4. To verify that all transition states corresponded to the appropriate minima, intrinsic reaction coordinate (IRC)[14] calculations were performed. These calculations established the minimum energy path between all *reactants* and *products*.
5. As many of the transition states involved bond formation and breaking, electron correlation effects were predicted to be important. Single-point energy calculations were, therefore, carried out on the RHF-optimized structures. These calculations were performed with second-order Møller–Plesset (MP2)[15] perturbation theory using the 6-31 + G(d) and aug-cc-pVDZ[16] bases. Only valence electrons were correlated in these calculations; that is, the frozen-core (fc) approximation was employed.
6. Solvation effects were calculated with the integral equation formalism of the polarizable continuum model (IEF-PCM)[17] by computing RHF single-point energies with the 6-31 + G(d) basis. Cavitation energies were computed via the method of Pierotti and Claverie,[18] while repulsion and dispersion energies were determined by the procedure of Amovilli and Mennucci.[19] Solute electron charge density that escaped from the solvent cavity was explicitly treated by the method of Mennucci and Tomasi.[20] H_2O was used as the solvent.

All calculations were performed with the GAMESS program[21] on a small Beowulf cluster of personal computers.

RESULTS AND DISCUSSION

Gas phase

The protonation of epihalohydrins can occur in principle at two sites: the oxygen (O) or the halogen (X = Cl, Br) atoms. Theoretical proton affinities (PA) and gas-phase basicities (GB) for protonation at these two sites have been computed and they are reported in Table 1. The PA and GB correspond to the change in the respective enthalpies (ΔH) and Gibbs free energies (ΔG) for the reactions given in Eqns 1 and 2.

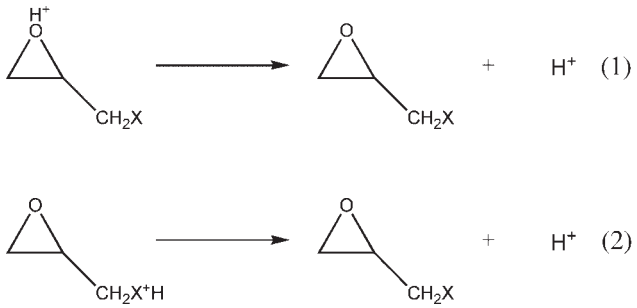

It is clear that protonation of the O atom is substantially preferred in both epihalohydrins: the greater the PA or GB, the more basic the site. Based upon these results, it is safe to assume that the epihalohydrins are protonated at the O atom of the epoxide ring under strongly acidic conditions.

Six possible conformers can result upon protonation of epihalohydrins at the O atom (**II**–**VII**). The lowest energy conformer (**II**) has the proton *cis* the halomethylene group (CH_2X) and the halogen atom in a gauche (−) orientation (**EXH$^+$**). (All referenced structures are illustrated in Fig. 1). At 298 K and 1 atm, this low energy conformer accounts for 99.5% of the Boltzmann distribution of protonated epichlorohydrins and 99.4% of the epibromohydrins.

The stability of **II** results primarily from electrostatic and polarization interactions between the proton on the O atom and the halogen atom, which is only possible

DOI: 10.1002/poc

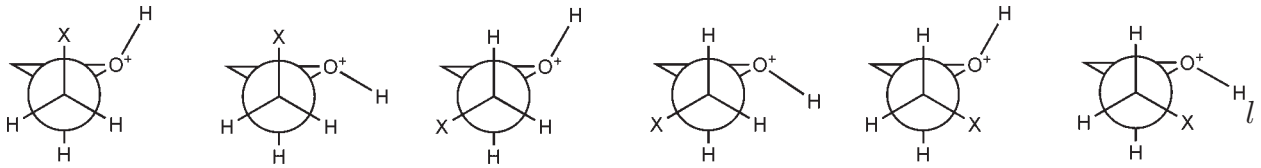

II III IV V VI VII

Table 1. Proton affinities (PA) and gas-phase basicities (GB) for epihalohydrins, 2,3-dihydroxy-1-halopropanes, 2,3-epoxy-1-hydroxypropane, 2-hydroxyoxetane, glycerol, and water in kcal mol^{-1}. Level of theory: MP2/aug-cc-pVDZ//HF/6-31 + G(d)

Compound	Site of protonation	PA	GB
Epichlorohydrin	O	186.0	178.2
	Cl	159.3	152.5
Epibromohydrin	O	186.9	179.2
	Br	162.6	155.7
2,3-Dihydroxy-1-chloro-propane	Cl	170.4	162.7
	2-OH	189.0	180.7
	3-OH	185.7	177.6
2,3-Dihydroxy-1-bromo-propane	Br	168.3	161.4
	2-OH	188.4	180.8
	3-OH	190.2	182.3
2,3-Epoxy-1-hydroxypropane	Epoxy O	193.1	185.6
	OH	184.8	177.2
2-Hydroxyoxetane	Oxetane O	192.7	186.5
	OH	177.2	169.9
Glycerol	1-OH	207.7 (209.1)[a]	199.4 (196.0)[a]
	2-OH	204.3 (209.1)[a]	196.3 (196.0)[a]
Water		162.6 (165.0)[a]	155.2 (157.7)[a]

[a] Experimental values: Hunter EP, Lias SG. *J. Phys. Chem. Ref. Data* 1998; 27: 413–656.

for the *cis* structures and is greatest for the gauche (−) orientation.

In the current study, H_2O served as the archetypal hard nucleophile. The driving energy for the reaction between H_2O and the protonated epihalohydrins is the formation of an ion-molecule (IM) complex. The structure results from the formation of a hydrogen bond between the O atom of the H_2O molecule and the proton on the epoxy O atom of the epihalohydrin (**IM1a**). The formation of the complex is both exothermic and exergonic (see Table S1 in the Supplementary Information), with similar complexation energies for the two-protonated epihalohydrins (ΔH: Cl = −20.7 *vs.* Br = −19.7 kcal mol^{-1}; ΔG: Cl = −12.4 *vs.* Br = −11.4 kcal mol^{-1}).

Nucleophilic attack can occur in principle at three sites in the protonated epihalohydrins: the C1 methylene, C2 methine, or C3 methylene positions. No transition state was found for the direct displacement of X^- by H_2O in the gas phase (Eqn 3).

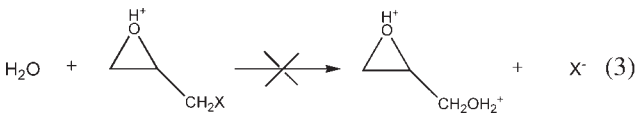

(3)

This is not too surprising as separated dicationic and anionic products would be formed in the absence of a mitigating polar solvent. This problem of charge separation can be overcome if the proton on the epoxy O atom is transferred to the halide-leaving group during the attack by H_2O at the C1 position (Eqn 4).

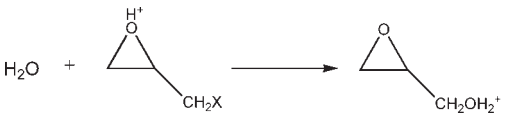

(4)

Just such a transition state was located for epichlorohydrin (**TS1a**). The enthalpy and free energy of activation for this C1 pathway were endothermic ($\Delta H^{\ddagger} = 13.7$ kcal mol^{-1}) and endergonic ($\Delta G^{\ddagger} = 21.2$ kcal mol^{-1}), respectively. These values are consistent with the lower PA and GB values for the chloro position of epichlorohydrin (Table 1). The imaginary frequency associated with this structure was found to be only 73 cm^{-1}, indicating a rather *loose* (i.e., entropically less demanding) transition state. An analogous transition state was found for epibromohydrin, where the enthalpy and free energy of activation were also positive: $\Delta H^{\ddagger} = 23.4$ and $\Delta G^{\ddagger} = 29.9$ kcal mol^{-1}. Once again, a small imaginary frequency of 127 cm^{-1} was found for this transition state. It may be concluded, therefore, that the attack by H_2O at the C1 position of epihalohydrins is unlikely in the gas phase, even with the accompanying loss of HX instead of X^-. If such an attack were possible,

DOI: 10.1002/poc

proton transfer from the hydroxy group to the epoxy O atom is predicted to be barrierless (Eqn 5); that is, the transition state (TS1b) is an energy maximum along the HF reaction coordinate, but it is not when it is corrected for electron correlation at the MP2 level.

(5)

The result of said proton transfers are IM complexes with enthalpies and free energies lower than those of the separated starting materials. These complexes should largely dissociate in the gas phase to yield protonated 2,3-epoxy-1-hydroxypropane (**P1**) and the respective hydrohalogenic acid, HX. The complete C1 mechanism is presented in Scheme 1, and the associated free energy reaction coordinate is given in Fig. 2.

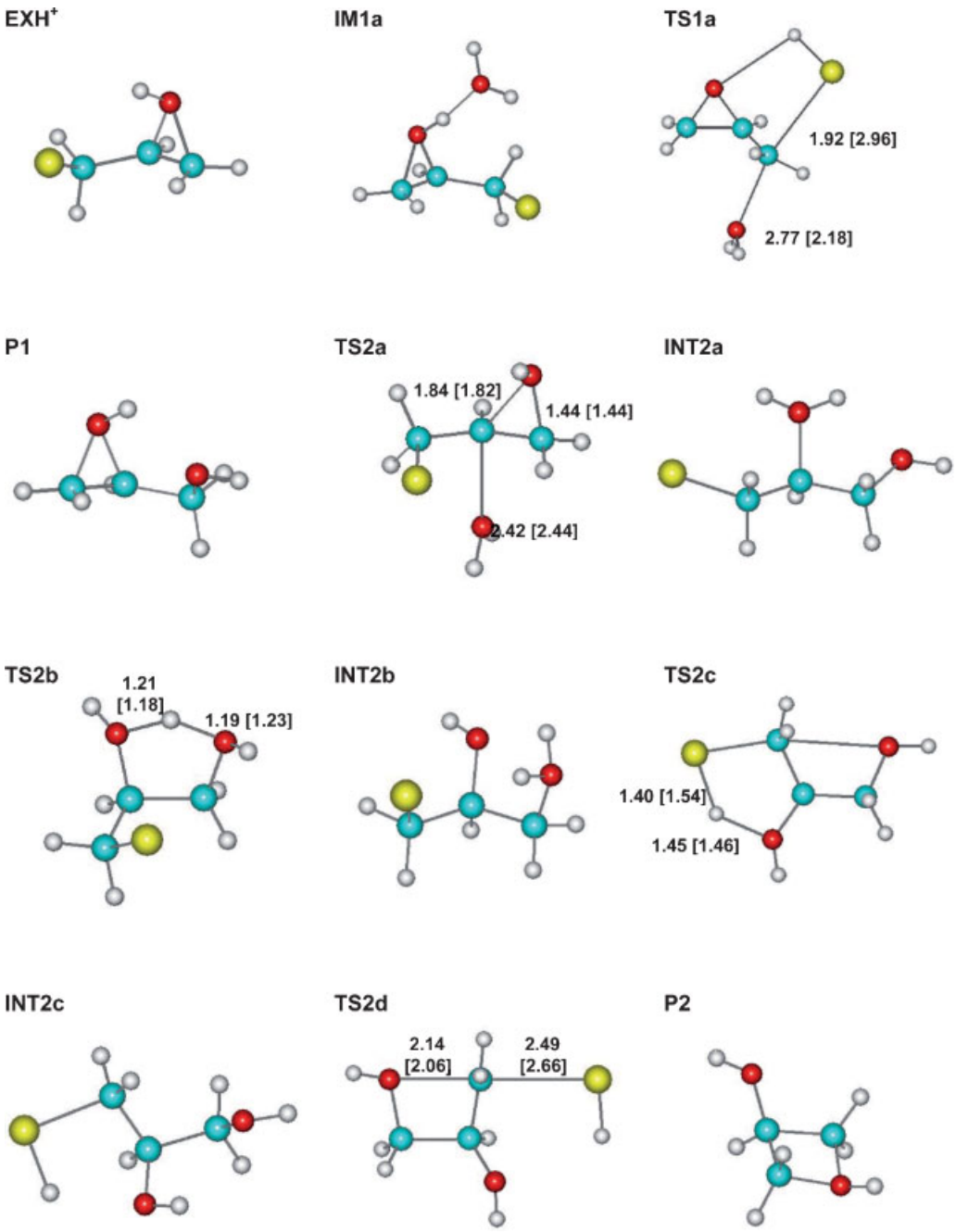

Figure 1. Illustrations of minimum-energy and transition-state structures discussed in the text. Atom colors: blue = carbon; white = hydrogen; red = oxygen; and yellow = chlorine or bromine. Bond distances in Å: chloro compounds, bold; bromo compounds, brackets

DOI: 10.1002/poc

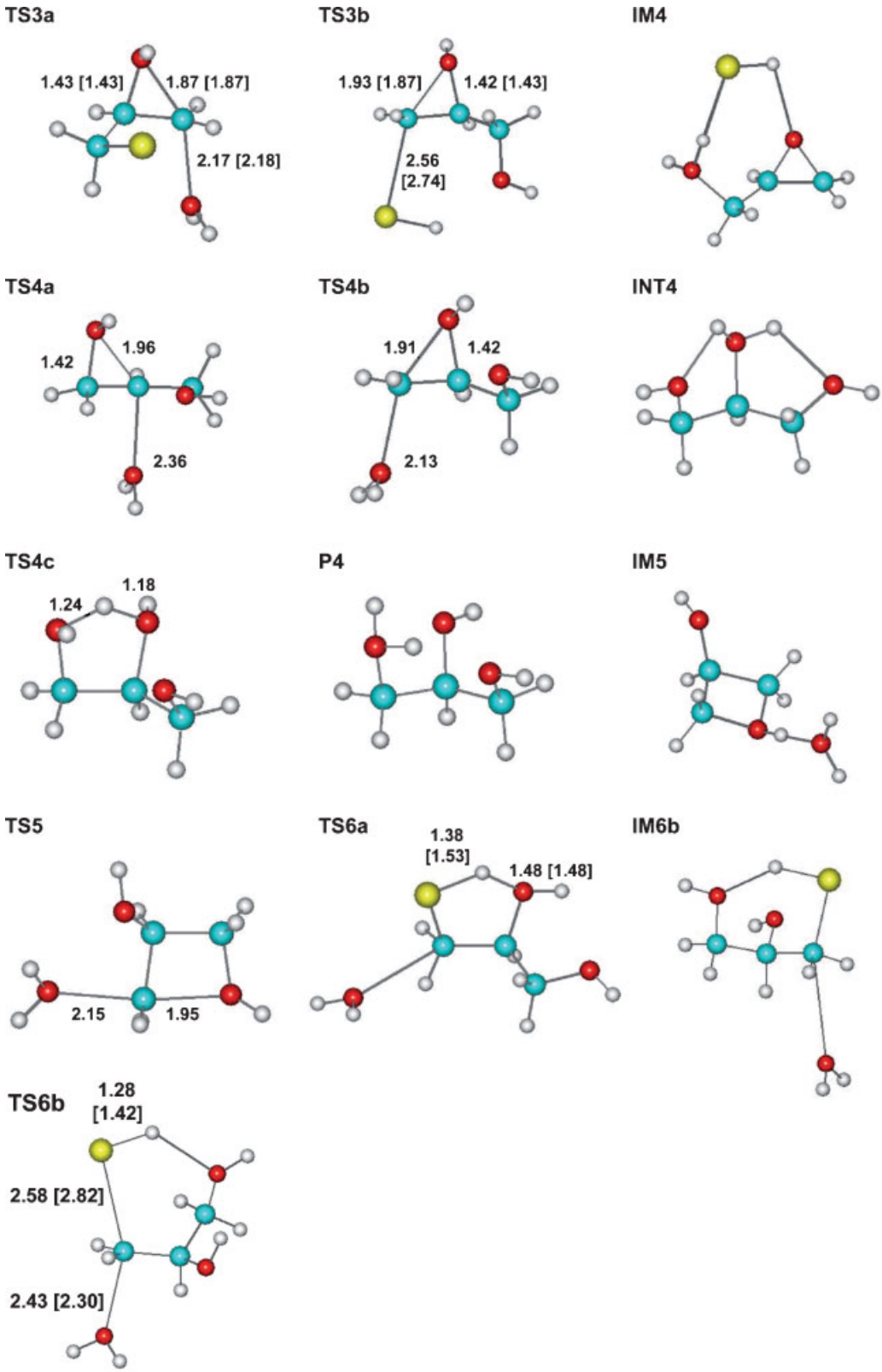

Figure 1. (*Continued*)

A transition state (**TS2a**) was found for attack by H_2O at the C2 position (Eqn 6). Both the chloro and bromo transition states possess enthalpies that are negative (Table S2) with respect to the separated reactants: $\Delta H_{Cl} = -4.4$ and $\Delta H_{Br} = -3.8\,\text{kcal mol}^{-1}$. The similarity of these transition states is reflected in their respective imaginary frequencies along the reaction coordinates: $\nu_{Cl} = 246$ and $\nu_{Br} = 247\,\text{cm}^{-1}$. The free energies for these two

DOI: 10.1002/poc

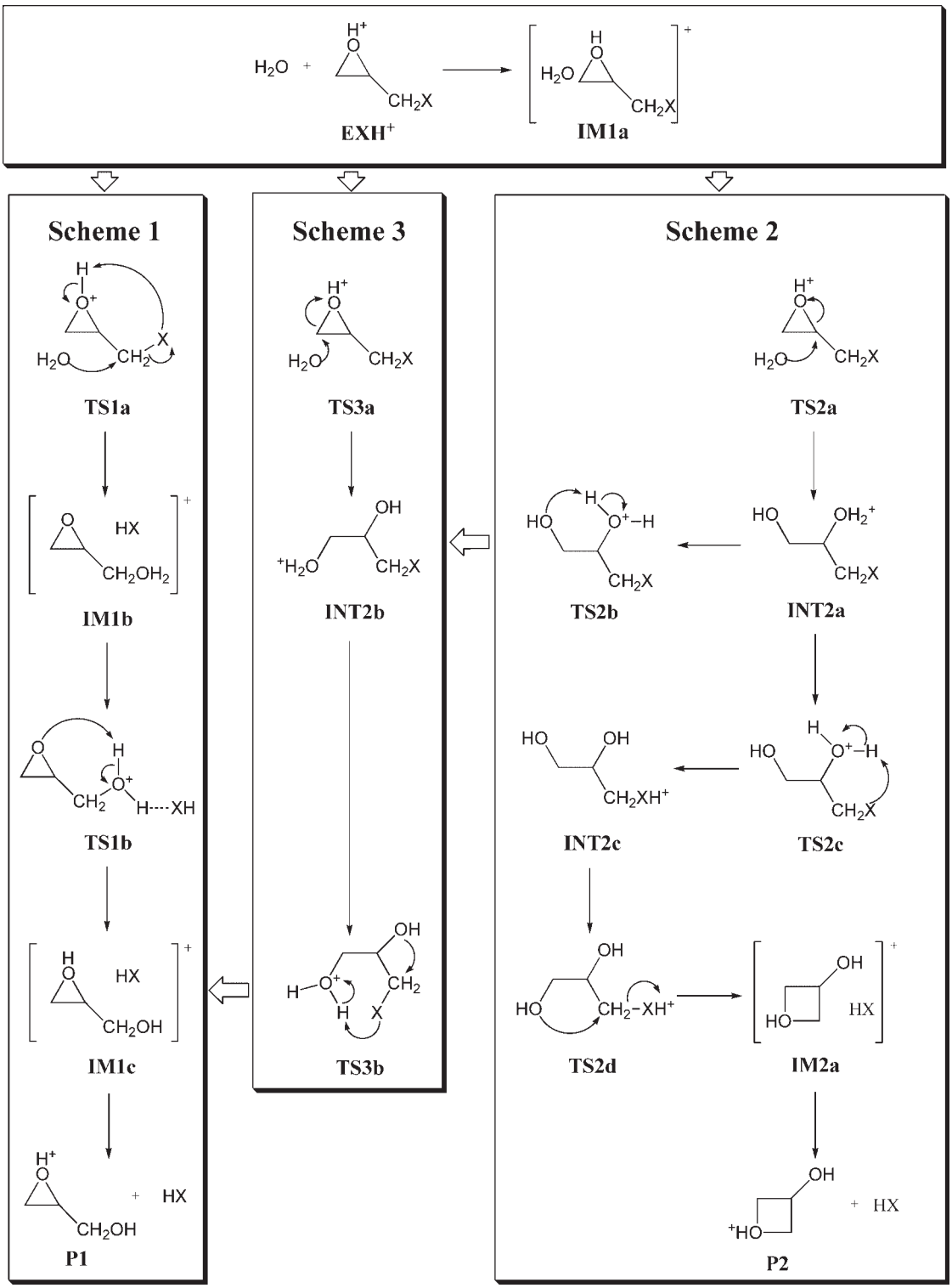

Schemes 1–3.

transition state are, however, higher in energy than the separated reactants: $\Delta G_{Cl} = 3.7$ and $\Delta G_{Br} = 4.4\,kcal\,mol^{-1}$. Nucleophilic attack results in the opening of the epoxide ring to form an intermediate, 2,3-dihydroxy-1-halopropane (**INT2a**), which is protonated at the C2 hydroxy group. The formation of this protonated intermediate is highly exothermic ($\Delta H_{Cl} = -28.1$ and $\Delta H_{Br} = -26.6\,kcal\,mol^{-1}$) and exergonic ($\Delta G_{Cl} =$

DOI: 10.1002/poc

-17.5 and $\Delta G_{Br} = -16.2\,kcal\,mol^{-1}$). Nucleophilic attack by H_2O at the C2 position is, therefore, predicted to be possible in the gas phase.

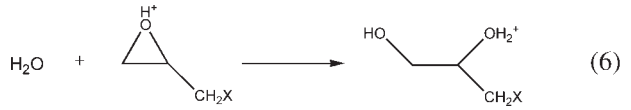

(6)

Transition states for attack by H_2O at the C3 position (**TS3a**) were also located (Eqn 7 and Table S3). Like the transition states for nucleophilic attack at the C2 positions, those for attack at the C3 positions are also exothermic ($\Delta H_{Cl} = -6.7$ and $\Delta H_{Br} = -6.2\,kcal\,mol^{-1}$) and slightly endergonic ($\Delta G_{Cl} = 2.2$ and $\Delta G_{Br} = 2.8\,kcal\,mol^{-1}$). Once again, the similarity of the transition states can be seen in the similar imaginary frequencies along the reaction coordinate: $\nu_{Cl} = 300$ and $\nu_{Br} = 302\,cm^{-1}$. The result of attack by H_2O at the C3 position is the formation of another intermediate, 2,3-dihydroxy- 1-halopropane (**INT2b**), this time protonated at the C3 hydroxy group. This ring-opening step is also exothermic ($\Delta H_{Cl} = -24.8$ and $\Delta H_{Br} = -28.4\,kcal\,mol^{-1}$) and exergonic ($\Delta G_{Cl} = -14.4$ and $\Delta G_{Br} = -17.7\,kcal\,mol^{-1}$), and it is, therefore, predicted to be viable in the gas phase.

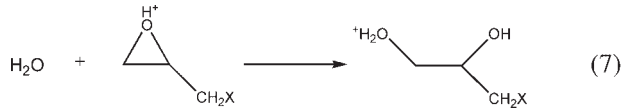

(7)

Interconversion between the two intermediates **INT2a** and **INT2b** (Eqn 8) is accomplished via intramolecular proton transfer (**TS2b**).

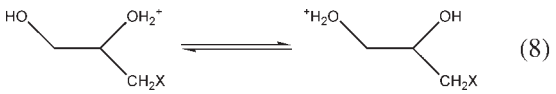

(8)

For both the chloro and bromo systems, the enthalpies and free energies for the transition states are lower in energy than the separated reactants: $\Delta H_{Cl} = -27.7$ *versus* $\Delta H_{Br} = -28.1\,kcal\,mol^{-1}$; $\Delta G_{Cl} = -16.5$ *versus* $\Delta G_{Br} = -16.7\,kcal\,mol^{-1}$. For the chloro compounds, the intermediate protonated at the C2 hydroxy group is lower in enthalpy ($\Delta\Delta H = -3.3\,kcal\,mol^{-1}$) and free energy ($\Delta\Delta G = -3.1\,kcal\,mol^{-1}$) than its C3 counterpart. The situation is reversed for the bromo compounds, where the intermediate protonated at the C3 hydroxy group possesses a lower enthalpy ($\Delta\Delta H = -1.8\,kcal\,mol^{-1}$) and free energy ($\Delta\Delta G = -1.5\,kcal\,mol^{-1}$). These thermodynamic differences are reflected in the imaginary frequencies along the reaction coordinate: $\nu_{Cl} = 1340$ and $\nu_{Br} = 1274\,cm^{-1}$. It should be noted that correcting the transition state (TS2b) for electron correlation at the MP2 level does not yield an energy maximum along the reaction coordinate. This mirrors the earlier result for TS1b, and it foreshadows those for TS2c.

Loss of X^- from the protonated intermediates can in principle be affected via ring closure; that is, via an intramolecular S_N2-type reaction. As was seen for the C1 mechanism, problems associated with the separation of charge in the products must be overcome. In the case of the intermediate protonated at the C2 hydroxy group (**INT2a**), ring closure with the loss of HX would result in the formation of an oxetane (Eqn 9). Attempts to locate a concerted transition state for this process proved unsuccessful. Instead, a transition state for the transfer of a proton from the hydroxy group to the halogen (**TS2c**) was found. While the barriers to proton transfer were lower in enthalpy and free energy than the separated reactants (ΔH: Cl $= -11.3$ and Br $= -11.5\,kcal\,mol^{-1}$; ΔG: Cl $= -0.5$ and Br $= -0.6\,kcal\,mol^{-1}$), the resulting 2,3-dihydroxy-1-halopropanes protonated at the halogen (**INT2c**) were calculated to have free energies greater than the separated reactants (ΔG: Cl $= 0.4$ and Br $= 3.2\,kcal\,mol^{-1}$); the enthalpies were, however, still predicted to be less than the separated reactants (ΔH: Cl $= -9.5$ and Br $= -6.5\,kcal\,mol^{-1}$). It is worth noting that the specific halogen had little impact on the respective imaginary frequencies along the reaction coordinates ($\nu_{Cl} = 814$ *vs.* $\nu_{Br} = 860\,cm^{-1}$).

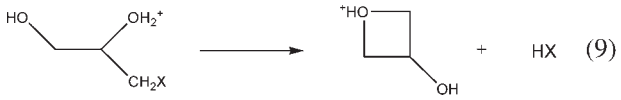

(9)

Regardless of the energetics for the proton transfer step, the transition state for the ring closure to form the oxetane with the loss of HX (**TS2d**) are endothermic (ΔH: Cl $= 9.8$ and Br $= 11.1\,kcal\,mol^{-1}$) and endergonic (ΔG: Cl $= 18.7$ and Br $= 19.6\,kcal\,mol^{-1}$). Such a mechanism is, therefore, highly unlikely in the gas phase, even though the formation of the resulting IM complex (protonated hydroxyoxetane + hydrohalogenic acid) is energetically favorable. Finally, the chloro mechanism for the formation of the oxetane is exothermic and exergonic, but it is not for the bromo pathway. The complete C2 mechanism is given in Scheme 2, and the corresponding free energy reaction coordinate is illustrated in Fig. 3.

It is also possible to reform an epoxide with the loss of HX from the intermediate protonated at the C3 hydroxy group (Eqn 10). Unlike the above pathway for the formation of an oxetane, a transition state for the simultaneous formation of the epoxide with the loss of HX was located (**TS3b**). This transition state was found to be endothermic (ΔH: Cl $= 6.7$ and Br $= 8.8\,kcal\,mol^{-1}$) and endergonic (ΔG: Cl $= 16.0$ and Br $= 18.0\,kcal\,mol^{-1}$) with roughly comparable imaginary frequencies ($\nu_{Cl} = 243$ *vs.* $\nu_{Br} = 274\,cm^{-1}$). The formation of the IM complexes was found to be exothermic; the formation of the chloro complex was also determined to be exergonic, but the bromo complex

DOI: 10.1002/poc

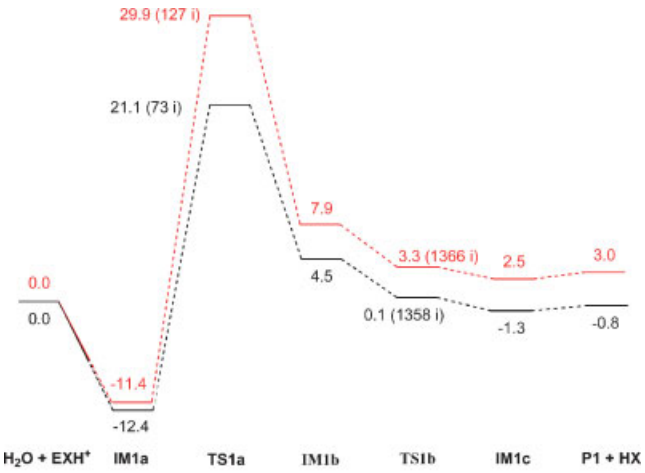

Figure 2. Free energy reaction coordinate for nucleophilic attack by water on protonated epichlorohydrin (black) and epibromohydrin (red) at the C1 position in kcal mol^{-1}. Parenthetical values: vibrational frequencies in cm^{-1}

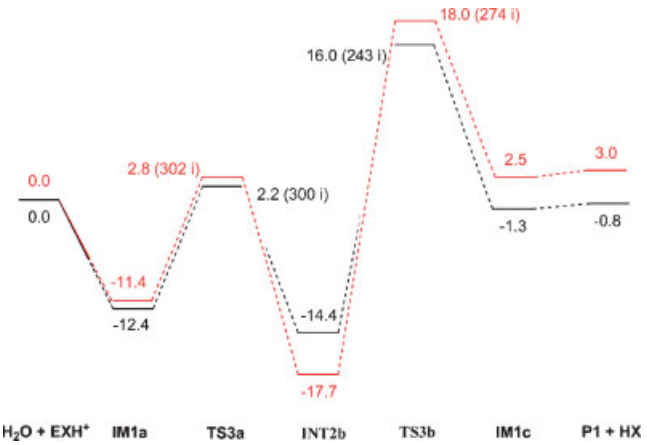

Figure 4. Free energy reaction coordinate for nucleophilic attack by water on protonated epichlorohydrin (black) and epibromohydrin (red) at the C3 position in kcal mol^{-1}. Parenthetical values: vibrational frequencies in cm^{-1}

was once again found to be endergonic.

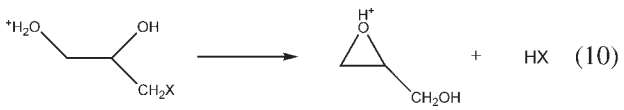

(10)

The overall mechanism for the reformation of an epoxide was found to be energetically favorable for the chloro compound but slightly less so for the bromo species. Intramolecular ring-closure is, nevertheless, predicted to be unlikely in the gas phase. The complete C3 pathway is provided in Scheme 3, and the associated free energy reaction coordinate can be found in Fig. 4.

Upon formation of protonated 2,3-epoxy-1-hydroxypropane (**P1**) or 2-hydroxyoxetane (**P2**), both ring structures are subject to further nucleophilic attack by H_2O (Eqns 11 and 12) leading to protonated glycerols.

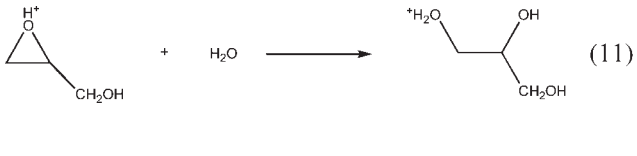

(11)

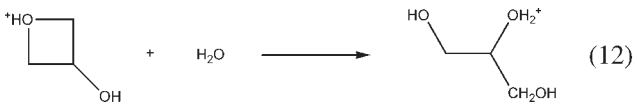

(12)

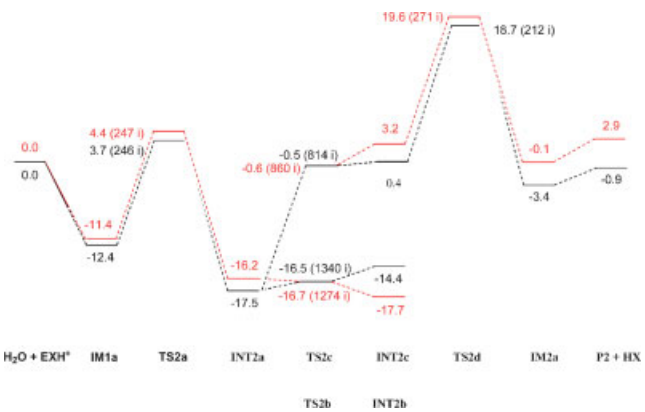

Figure 3. Free energy reaction coordinate for nucleophilic attack by water on protonated epichlorohydrin (black) and epibromohydrin (red) at the C2 position in kcal mol^{-1}. Parenthetical values: vibrational frequencies in cm^{-1}

These two pathways are outlined in Schemes 4 and 5, respectively. The driving force behind these two mechanisms is, once again, the formation of IM complexes between H_2O and the epoxide (**IM4a**) or oxetane (**IM5a**), both of which are exothermic and exergonic in nature.

Two transition states for attack by H_2O on the epoxide were located, one for the C2 position (**TS4a**) and the other for the C3 position (**TS4b**). Both transition states are exothermic, with attack at the C3 position being favored (ΔH: **TS4a** $= -2.1$ *vs.* **TS4b** $= -4.4$ kcal mol^{-1}; see Table S4 in the Supplementary Information). The transition state corresponding to attack at the C2 position is somewhat less demanding entropically as revealed by the imaginary frequencies along the reaction coordinates ($\nu_{\mathbf{TS4a}} = 183$ *vs.* $\nu_{\mathbf{TS4b}} = 295$ cm^{-1}). While both transition states are marginally endergonic, the one for attack at the C3 position is again slightly favored (ΔG: **TS4a** $= 5.9$ *vs.* **TS4b** $= 4.5$ kcal mol^{-1}).

Nucleophilic attack at either site results in the formation of protonated glycerols; in the case of attack at the C2 position, a glycerol protonated at the C2 hydroxy group is formed, while a protonated glycerol at the C1 hydroxy group is formed in the attack at the C3

DOI: 10.1002/poc

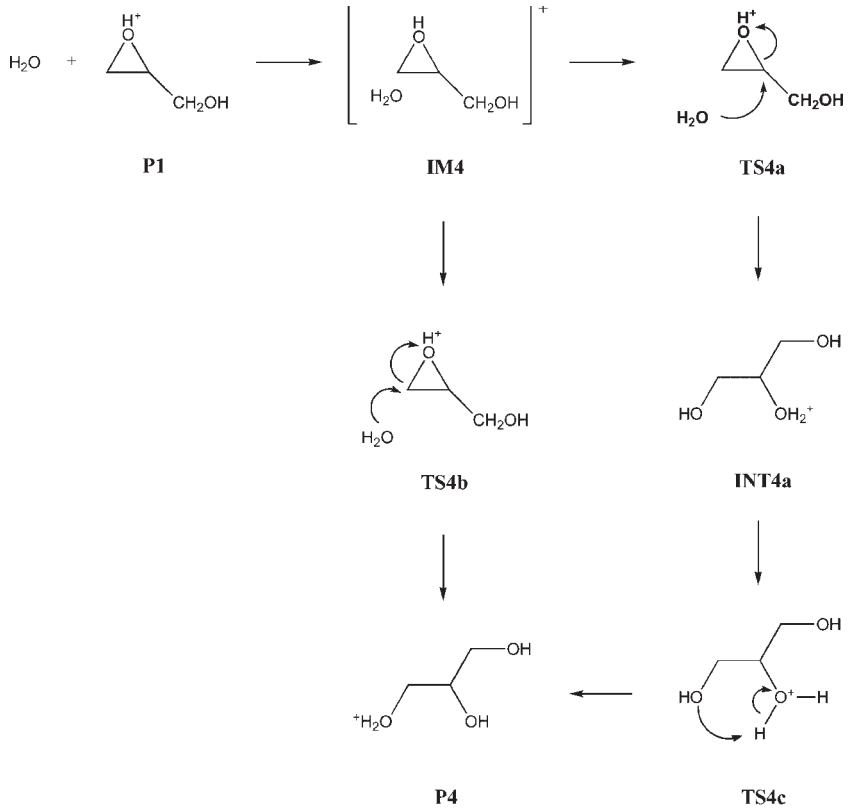

Scheme 4.

position. Both products are lower in energy than the separated reactants, and the product of C3 attack is slightly more stable than that resulting from C2 attack. This fact is also reflected in the computed PA and GB for glycerol (Table 1). The two protonated glycerols are readily interconverted via a transition state involving proton transfer (**TS4c**), the enthalpy and free energy of which are lower than those for the separated reactants ($\Delta H = -27.4$ and $\Delta G = -15.9\,\text{kcal mol}^{-1}$).

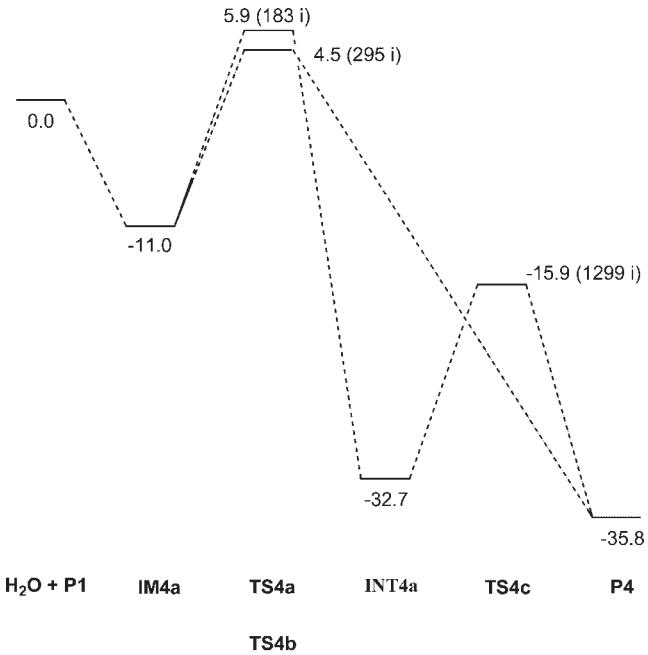

Figure 5. Free energy reaction coordinate for nucleophilic attack by water on protonated 2,3-epoxy-1-hydroxypropane in kcal mol^{-1}. Parenthetical values: vibrational frequencies in cm^{-1}

A complete reaction coordinate for Scheme 4 is given in Fig. 5. It is possible to conclude from this reaction coordinate that, if 2,3-epoxy-1-hydroxypropane were to be formed in the gas phase, it would quickly undergo a ring opening via nucleophilic attack by H_2O at either the C2 or C3 positions to form the more stable protonated glycerol (**P4**).

Nucleophilic attack by H_2O on the oxetane can also occur, in this case at the C2 (or equivalent C4) position. This mechanism is outlined in Scheme 5. The transition state for this attack (**TS5a**) is also enthalpically favored ($\Delta H = -2.2\,\text{kcal mol}^{-1}$), but it is unfavorable in terms its free energy ($\Delta G = 7.9\,\text{kcal mol}^{-1}$). This transition state is also slightly more demanding entropically ($\nu = 355\,\text{i cm}^{-1}$). Nucleophilic attack at the C2 position leads to the formation of the less stable protonated glycerol (**INT4a**). This species can, once again, be readily interconverted to the more stable protonated glycerol (**P4**) via proton transfer between the C1 and C2 hydroxy groups. The complete reaction coordinate for this mechanism is given in Fig. 6 (see also Table S5 in the Supplementary Information). It may again be concluded that if the hydroxyoxetane were to form in the gas phase, it would undergo rapid ring opening via nucleophilic

DOI: 10.1002/poc

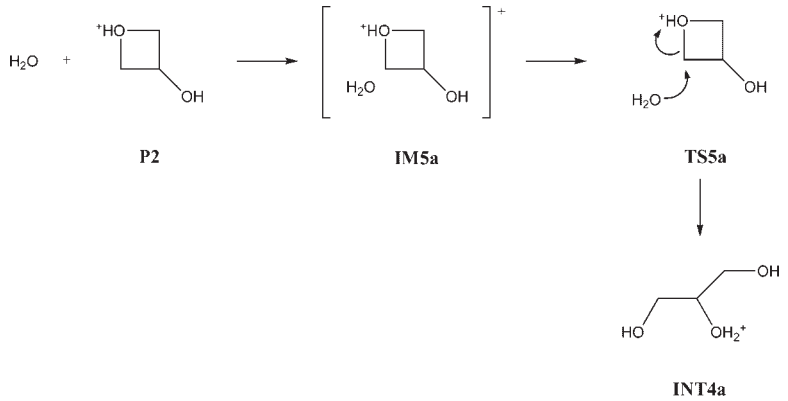

Scheme 5.

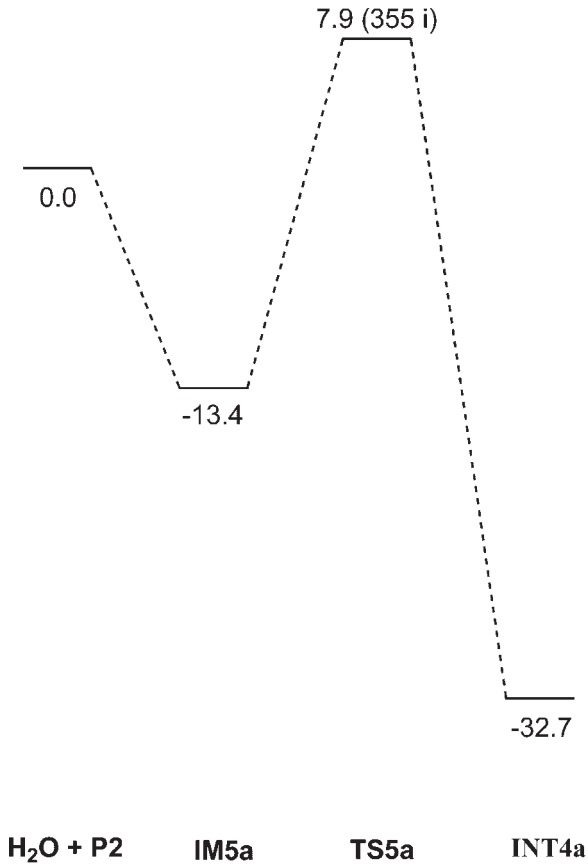

Figure 6. Free energy reaction coordinate for nucleophilic attack by water on protonated 2-hydroxyoxetane in kcal mol^{-1}. Parenthetical values: vibrational frequencies in cm^{-1}

attack by H_2O to form the most stable protonated glycerol.

The global minima resulting from attack by H_2O on the protonated epihalohydrins are protonated 2,3-dihydroxy-1-halopropanes, with the chloro compound protonated at the C2 hydroxy group (**INT2a**) and the bromo species protonated at the C3 hydroxyl group (**INT2b**). Both intermediates may be subject to further attack by H_2O to displace the halide and form a protonated glycerol. Once again, direct displacement of the halide is energetically unfavorable in the gas phase as it leads to a large separation of charge. This problem is partially overcome by transferring a proton from the protonated hydroxy group to the halogen (**TS6a**). This step is endothermic ($\Delta H = 6.1$ kcal mol^{-1}) and endergonic ($\Delta G = 12.9$ kcal mol^{-1}) with respect to the separated reactants (H_2O and **INT2a**) for the chloro species (Table S6). The resulting IM complex (**IM6b**) is higher in energy still. Actual displacement of HCl by H_2O occurs via an S_N2-type transition state (**TS6b**), which is even more energetically unfavorable ($\Delta H = 23.9$ and $\Delta G = 31.1$ kcal mol^{-1}). The formation of the products (**P4** and HCl) is, however, appreciably exothermic ($\Delta H = -20.0$ kcal mol^{-1}) and exergonic ($\Delta G = -19.1$ kcal mol^{-1}) (Scheme 6).

A comparable pathway for the **INT2b** bromo compound was not found, but one for the **INT2a** intermediate was located. This pathway is remarkably similar to that for the chloro compound: the rate-determining transition state (**TS6b**) is very energetically unfavorable in the gas phase ($\Delta H = 27.8$ and $\Delta G = 35.0$ kcal mol^{-1}), while the overall reaction is both exothermic and exergonic ($\Delta H = -15.9$ and $\Delta G = -15.1$ kcal mol^{-1}).

From these reaction coordinates, it is clear that formation of (protonated) glycerol in the gas phase from reaction of H_2O with epihalohydrins is not likely, the predicted products should simply be 2,3-dihydroxy-1-halopropanes, even though the overall reaction (Eqn 13) is calculated to be highly exothermic (ΔH: Cl $= -48.1$ and Br $= -44.2$ kcal mol^{-1}) and exergonic (ΔG: Cl $= -36.6$ and Br $= -32.3$ kcal mol^{-1}).

(13)

Aqueous solution

The impact of aqueous solvation upon the gas-phase reaction coordinates was assessed through an additional

DOI: 10.1002/poc

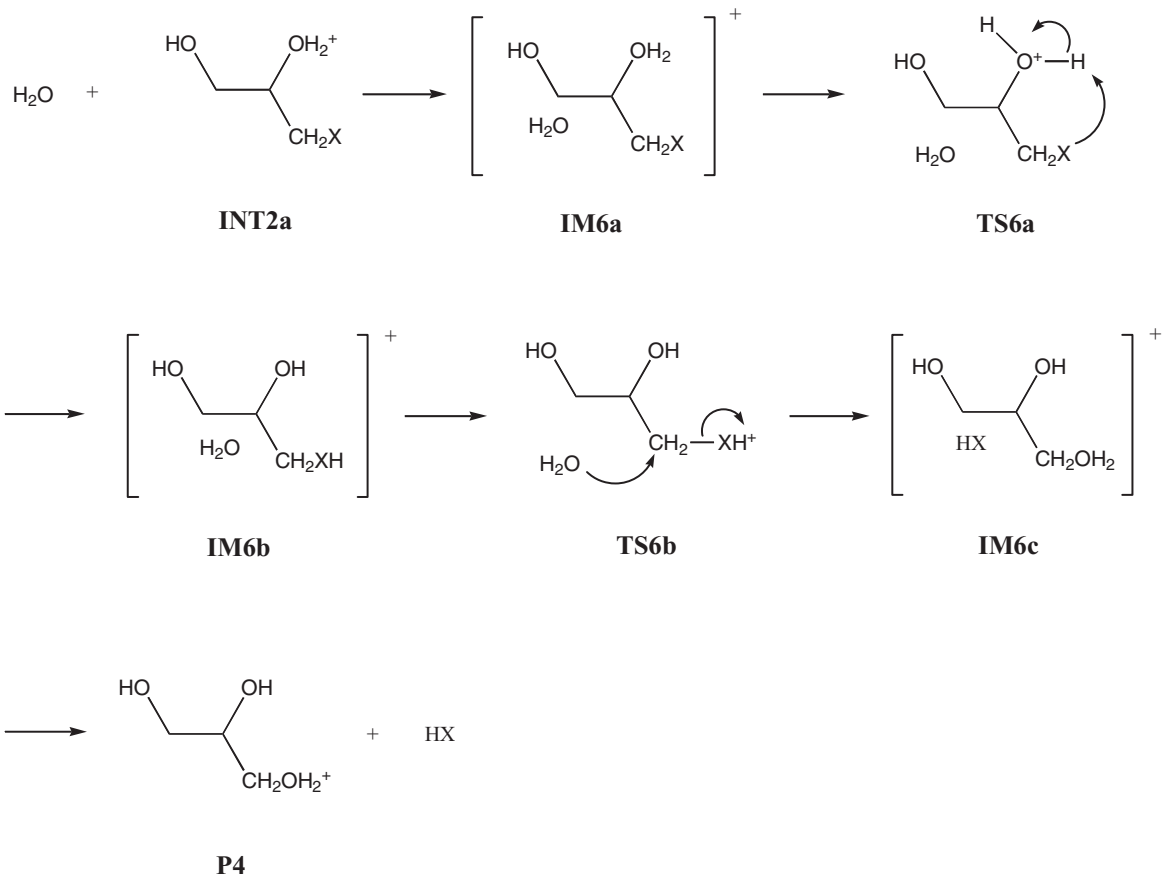

Scheme 6.

series of calculations at the Hartree–Fock (HF) level of theory with the polarizable continuum model (PCM). Specifically, HF-PCM/6-31 + G(d) single-point energy calculations were carried out on all stationary points. From these calculations, the free energies of hydration were determined. These free energies of hydration are the sum of a number of individual energy contributions: the change in internal energy upon reorganization of the electronic wavefunction in going from the gas phase to solution (ΔE); electrostatic interactions (ES); cavitation (CAV); dispersion (DIS); and repulsion (REP). (These individual values and their sums may be found in Table S7 in the Supplementary Information.) The free energies in H_2O were obtained by adding the hydration free energies to those determined in the gas phase, and these hydration free energies are given in Table 2.

With the exceptions of HCl and HBr, hydration is a stabilizing influence on all the species examined. While both the ES and DIS energy contributions are stabilizing, with ES interactions about five times larger than DIS interactions. The other energy contributions (ΔE, CAV, and REP) are all destabilizing. It is worth noting that the magnitudes of these contributions are remarkably similar over all compounds; for example, the REP values all average between three and four kilocalories per mole. They are also largely mitigated by the stabilizing DIS contribution. The differences between the gas-phase and aqueous reaction coordinates can, therefore, be explained to a first approximation by electrostatic effects. This is not too surprising given that most of the species are charged or possess large dipole moments.

For attack by H_2O at the C1 position of the epihalohydrins, the free energies for the rate-determining step (**TS1a**) have substantially increased over those for the gas phase. ($\Delta\Delta G$: Cl = 14.7 and Br = 12.9 kcal mol^{-1}). In a similar fashion, the overall reaction has become more endergonic ($\Delta\Delta G$: Cl = 8.5 and Br = 6.1 kcal mol^{-1}). Both of these changes may be attributed to greater stabilization of the reactants than the rate-determining transition states and products. It may, therefore, be concluded that aqueous solvation should retard the C1 mechanism.

Similar results were obtained for the pathway associated with attack by H_2O on the C2 position of the epihalohydrins. Here, the barriers (**TS2a**) have increased by comparable amounts to that seen for the C1 pathway ($\Delta\Delta G$: Cl = 13.2 and Br = 12.7 kcal mol^{-1}). The barriers to proton transfer between the hydroxy groups (**TS2b**) are still found to be exergonic, while those for proton transfer to the halogen (**TS2c**) are now endergonic. The free energies associated with the intramolecular S_N2 step to form an oxetane with the loss of HX (**TS2d**) have also increased markedly ($\Delta\Delta G$: Cl = 12.7 and Br = 12.2 kcal mol^{-1}), and the overall reactions have become marginally more endergonic. Aqueous solvation

DOI: 10.1002/poc

Table 2. Aqueous free energies ($\triangle G_{aq}$) associated with Schemes 1–6 in kcal mol^{-1}. See text for computational details

Scheme 1

Halogen	$H_2O + \mathbf{EXH^+}$	**IM1a**	**TS1a**	**IM1b**	**TS1b**	**IM1c**	**P1** + HX
Cl	0.0	4.0	35.9	13.8	13.7	13.6	7.7
Br	0.0	1.5	42.8	16.9	15.0	16.8	9.1

Scheme 2

Halogen	$H_2O + \mathbf{EXH^+}$	**IM1a**	**TS2a**	**INT2a**	**TS2b**	**INT2b**
Cl	0.0	4.0	16.9	−10.1	−10.6	−11.7
Br	0.0	1.5	17.1	−10.6	−11.4	−11.1

Scheme 2

Halogen	**TS2c**	**INT2c**	**TS2d**	**IM2a**	**P2** + HX
Cl	10.2	11.0	31.4	7.3	3.2
Br	9.5	12.9	31.8	11.4	4.6

Scheme 3

Halogen	$H_2O + \mathbf{EXH^+}$	**IM1a**	**TS3a**	**INT2b**	**TS3b**	**IM1c**	**P1** + HX
Cl	0.0	4.0	12.1	−11.7	26.2	13.6	7.7
Br	0.0	1.5	12.5	−11.1	27.3	16.8	9.1

Scheme 4

$H_2O + \mathbf{P1}$	**IM4a**	**TS4a**	**INT4a**	**TS4b**	**TS4c**	**P4**
0.0	−5.1	16.0	−25.7	13.4	−10.2	−28.0

Scheme 5

$H_2O + \mathbf{P2}$	**IM5a**	**TS5a**	**INT4a**
0.0	1.3	21.3	−25.7

Scheme 6

Halogen	$H_2O + \mathbf{INT2a}$	**IM6a**	**TS6a**	**IM6b**	**TS6b**	**IM6c**	**P4** + HX
Cl	0.0	1.3	28.2	29.9	44.5	12.1	−10.2
Br	0.0	2.4	28.8	31.3	49.4	15.7	−6.8

has, therefore, rendered attack by H_2O at the C2 position of the epihalohydrins less likely and oxetane formation improbable.

For attack by H_2O at the C3 positions of the epihalohydrins, the reactants have once again been preferentially stabilized, albeit to a lesser degree. The free energies for the rate-determining transition states (**TS3a**) have only increased by 9.9 and 9.7 kcal mol^{-1} for the chloro and bromo pathways, respectively, in going from the gas phase to aqueous solution. The transition states for the reformation of the epoxides with the loss of HX (**TS3b**) have also increased by similar amounts ($\Delta\Delta G$: Cl = 10.2 and Br = 9.3 kcal mol^{-1}). As was seen for both the C1 and C2 pathways, the overall reaction has become more endergonic.

The impact of hydration upon ring opening of the reformed epoxide (**P1**) and newly formed oxetane (**P2**) were also investigated. For attack by H_2O on the epoxide, hydration has served merely to make the process less likely at both the C2 and C3 positions ($\Delta\Delta G$: **TS4a** = 10.1 and **TS4b** = 8.9 kcal mol^{-1}), with attack at the C3 position still favored, now by 2.6 kcal mol^{-1}. Proton transfer between the hydroxy groups of the nascent protonated glycerol is still exergonic, as is the overall reaction. The barrier to H_2O attack on the oxetane ring (**TS5a**) has increased even more in going from the gas

DOI: 10.1002/poc

Table 3. Gas phase (**bold**) and aqueous (*italics*) free energies of activations ($\triangle G^{\ddagger}$) and reaction ($\triangle_r G$) for the proposed mechanisms (Schemes 1–6) in kcal mol^{-1}. See text for computational details

Scheme	X	Reaction	$\triangle G^{\ddagger}$	$\triangle_r G$	Reaction	$\triangle G^{\ddagger}$	$\triangle_r G$
1	Cl	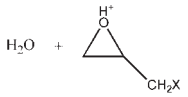	**21.2** *35.9*	**−0.8** *7.7*			
	Br	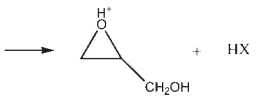	**29.9** *42.8*	**3.0** *9.1*			
2	Cl	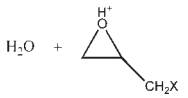	**3.7** *16.9*	**−17.5** *−10.1*	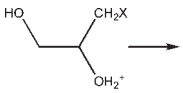	**18.7** *31.4*	−0.9 *3.2*
	Br	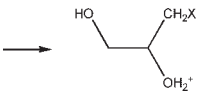	**4.4** *17.1*	**−16.2** *−10.6*	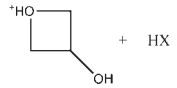	**19.6** *3.8*	**2.9** *4.6*
3	Cl	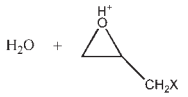	**2.2** *12.1*	**−14.4** *−11.7*	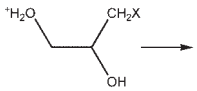	**16.0** *26.2*	**−0.8** *7.7*
	Br	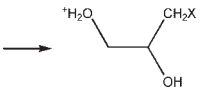	**2.8** *12.5*	**−17.7** *−11.1*	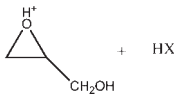	**18.0** *27.3*	**3.0** *9.1*
4		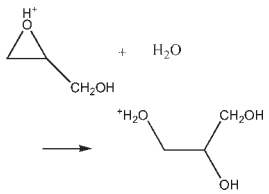	**5.9** *16.0*	**−35.8** *−28.0*			
5		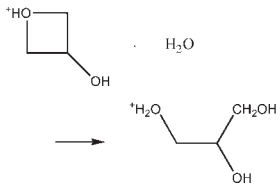	**7.9** *21.3*	**−32.7** *−25.7*			
6	Cl	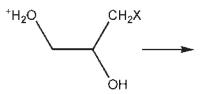	**31.1** *44.5*	**−19.1** *−10.2*			
	Br	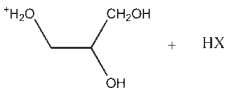	**35.0** *49.4*	**−15.1** *−6.8*			

phase to aqueous solution ($\Delta\Delta G = 13.4$ kcal mol^{-1}), although the reaction is still quite exergonic.

Finally, the impact of hydration upon the attack by H_2O on the 2,3-dihydroxy-1-halopropanes was explored. Once again, these pathways have become more unfavorable kinetically, where the rate-determining transition states (**TS6b**) have increased considerably ($\Delta\Delta G$: Cl = 13.4 and Br = 14.4 kcal mol^{-1}), as have the transition states (**TS6a**) leading to the precursor intermediate (**IM6b**).

CONCLUSIONS

A number of conclusions can be readily drawn regarding the reactivity of epihalohydrins under acidic conditions in the gas phase and aqueous solution. Both the gas phase

DOI: 10.1002/poc

and aqueous solution results are succinctly summarized in Table 3, where free energies of activation for the rate-determining steps ($\Delta G^{\ddagger}$) and reaction ($\Delta_r G$) are given for the proposed mechanisms.

Gas phase

1. Attack by H_2O at the C1 position of epihalohydrins is very unlikely, even with proton transfer from the oxygen atom of the epoxide ring to the halogen.
2. Attack by H_2O at the C2 and C3 positions is quite possible. Ring opening from the C3 position is, moreover, kinetically favored over that at the C2 position. The result of attack by H_2O at the epoxide ring is the formation of (protonated) 2,3-dihydroxy-1-halopropane intermediates.
3. Intramolecular S_N2 reactions to form a new epoxide or oxetane with concurrent loss of the appropriate hydrohalogenic acid is unlikely given the size of the barriers for these processes.
4. If said epoxide or oxetane were to form, they would be subject to ready nucleophilic attack on the rings by H_2O to form (protonated) glycerols.
5. The global minima of the potential energy surfaces are 2,3-dihydroxy-1-halopropanes, which are kinetically stable with respect to subsequent attack by H_2O to form (protonated) glycerols.

Aqueous solution

1. With the exceptions of two products (HCl and HBr), hydration stabilizes all of the stationary points on the gas-phase potential energy surfaces. This is accomplished primarily through electrostatic interactions between the dipolar solvent (H_2O) and the charged or dipolar species.
2. The reactants are preferentially solvated over the other species along the reaction coordinates. This has the effect of increasing the relative free energies of the minima and transition states.
3. The qualitative conclusions drawn from the gas-phase mechanisms are simply reinforced by aqueous solvation under acidic conditions; that is, attack by H_2O on the epihalohydrins is most likely at the C3 position followed by that at the C2 position, and it is unlikely at the C1 position; attack at the C3 and C2 positions should lead to 2,3-dihydroxy-1-halopropanes.

These results are in stark contrast to the reactivity of epihalohydrins under basic conditions. In a basic environment, nucleophilic attack at the C1 position is the preferred pathway in the gas phase for epibromohydrin, and it is competitive in polar solvents. This is because issues of charge separation do not arise for the direct displacement of the halides by hydroxide. Even nucleophilic attack at the C2 position is more favorable to that at the C1 position in acidic media. It is also important to note that the gas phase and aqueous transformation under acidic conditions are predicted to be slower than those under basic conditions. This may be attributed to the aforementioned issues involving charge separation and the fact that H_2O is a weaker nucleophile than hydroxide.

SUPPLEMENTARY INFORMATION

Complete gas-phase reaction enthalpies and free energies for the proposed mechanisms can be found in Tables S1–S6. Decomposition of the PCM free energies of hydration is given in Table S7. Cartesian coordinates are available upon request from the authors.

REFERENCES

1. (a) Merrill GN. *J. Phys. Org. Chem.* 2004; **17**: 241–248; (b) Merrill GN. *J. Phys. Org. Chem.* 2007; **20**: 19–29.
2. (a) Swern D, Billen GN, Knight HB. *J. Am. Chem. Soc.* 1949; **71**: 1152–1156; (b) Nichols PL Jr, Ingham JD. *J. Am. Chem. Soc.* 1955; **77**: 6547–6551.
3. McClure DE, Arison BH, Baldwin JJ. *J. Am. Chem. Soc.* 1979; **101**: 3666–3668.
4. Ohishi Y, Nakanishi T. *Chem. Pharm. Bull.* 1983; **31**: 3418–3423.
5. Cawley JJ, Onat E. *J. Phys. Org. Chem.* 1994; **7**: 395–398.
6. Whalen DF. *Tetrahedron Lett.* 1978; **50**: 4973–4976.
7. Politzer P, Laurrence PR. *Int. J. Quantum Chem. Biochem. Symp.* 1984; **11**: 155–166.
8. (a) Hall GG. *Proc. Roy. Soc. (London)* 1951; **A1951**: 541–552; (b) Roothaan CCJ. *Rev. Mod. Phys.* 1951; **23**: 69–89.
9. (a) Ditchfield R, Hehre WJ, Pople JA. *J. Chem. Phys.* 1971; **54**: 724–728; (b) Hehre WJ, Ditchfield R, Pople JA. *J. Chem. Phys.* 1972; **56**: 2257–2261; (c) Francl MM, Pietro WJ, Hehre WJ, Binkley JS, Gordon MS, DeFrees DJ, Pople JA. *J. Chem. Phys.* 1982; **77**: 3654–3665.
10. Hariharan PC, Pople JA. *Theor. Chim. Acta.* 1973; **28**: 213–222.
11. (a) Clark T, Chandrasekhar J, Spitznagel GW, Schleyer PvR. *J. Comp. Chem.* 1983; **4**: 294–301; (b) Spitznagel GW. Diplomarbeit, Erlangen, 1982.
12. McQuarrie DA. *Statistical Mechanics*. University Science Books: Sausalito, CA, 2000.
13. (a) Pople JA, Scott AP, Wong MW, Radom L. *Isr. J. Chem.* 1993; **33**: 345–350; (b) Scott AP, Radom L. *J. Phys. Chem.* 1996; **100**: 16502–16513.
14. Gonzales C, Schlegel HB. *J. Chem. Phys.* 1989; **90**: 2154–2161.
15. (a) Møller C, Plesset MS. *Phys. Rev.* 1934; **46**: 618–622; (b) Binkley JS, Pople JA. *Int. J. Quantum Chem.* 1975; **9**: 229–236; (c) Fletcher GD, Rendell AP, Sherwood P. *Mol. Phys.* 1997; **91**: 431–438.
16. (a) Dunning TH, Jr. *J. Chem. Phys.* 1989; **90**: 1007–1023; (b) Kendall RA, Dunning TH, Jr. *J. Chem. Phys.* 1992; **96**: 6769–6779.
17. Tomasi J, Persico M. *Chem. Rev.* 1994; **94**: 2027–2094.
18. (a) Pierotti RA. *Chem. Rev.* 1976; **76**: 717–726; (b) Langlet J, Claverie P, Caillet J, Pullman A. *J. Phys. Chem.* 1988; **92**: 1617–1631.
19. Amovilli C, Mennucci B. *J. Phys. Chem. B* 1997; **101**: 1051–1057.
20. Mennucci B, Tomasi J. *J. Chem. Phys.* 1997; **106**: 5151–5158.
21. Schmidt MW, Baldridge KK, Boatz JA, Jensen JH, Koseki S, Matsunaga N, Gordon MS, Nguyen KA, Su S, Windus TL, Elbert ST, Montgomery J, Dupuis M. *J. Comp. Chem.* 1993; **14**: 1347–1363.

DOI: 10.1002/poc